AMPA-sst2 somatostatin receptor interaction in rat hypothalamus requires activation of NMDA and/or metabotropic glutamate receptors and depends on intracellular calcium.

Stéphane Peineau, Brigitte Potier, Florence Petit, Pascal Dournaud, Jacques Epelbaum, Robert Gardette

INTERACTION BETWEEN AMPA-GLUTAMATE AND SST2-SOMATOSTATIN RECEPTORS IN RAT MEDIOBASAL HYPOTHALAMUS REQUIRES ACTIVATION OF NMDA AND/OR METABOTROPIC GLUTAMATE RECEPTORS AND DEPENDS ON INTRACELLULAR CALCIUM

. Stéphane Peineau[1], Brigitte Potier[1], Florence Petit, Pascal Dournaud, Jacques Epelbaum and Robert Gardette. INSERM U549, IFR Broca Sainte Anne, 2ter rue d'Alésia, 75014 Paris.

[1] : SP and BP contributed equally to this work Running title : Interactions between AMPA glutamate and sst2 SRIF receptors Key words : Glutamate receptor, Modulation, Somatostatin Section : Cell physiology

Summary

Modulation of glutamatergic transmission by neuropeptides is an essential aspect of neuronal network activity. Activation of the hypothalamic somatostatin sst2 receptor subtype by octreotide decreases AMPA glutamate responses, indicating a central link between a neurohormonal and neuromodulatory peptide and the main hypothalamic fast excitatory neurotransmitter. In mediobasal hypothalamic slices, sst2 activation inhibits the AMPA component of glutamatergic synaptic responses but is ineffective when AMPA currents are pharmacologically isolated. In mediobasal hypothalamic cultures, the decrease of AMPA currents induced by octreotide requires a concomitant activation of sst2 receptors with either NMDA and/or metabotropic glutamate receptors. This modulation depends on changes in intracellular calcium concentration induced by calcium flux through NMDA receptors or calcium release from intracellular stores following metabotropic glutamate receptor activation. These results highlight an unusual regulatory mechanism in which the simultaneous activation of at least three different types of receptors is necessary to allow somatostatin-induced modulation of fast synaptic glutamatergic transmission in the hypothalamus.

Since the first demonstration of the depressant action of leucine-enkephalin on glutamate-evoked responses (Barker et al., 1978), interactions between neuropeptides and amino acids have turned out to be a major regulatory mechanism in the control of neuronal excitability and

neuronal network activity. Neuropeptides affect particularly GABAergic or glutamatergic synapses by acting either pre- or postsynaptically. In the case of glutamatergic synapses, presynaptic effects lead to a depression or a facilitation of synaptic transmission, as shown recently for Neuropeptide Y (McQuiston and Colmers, 1996 ; Bijak, 2000) or Galanin (Mazarati et al., 2000), and for Thyrotropin-releasing hormone (Behbehani et al., 1990) or oxytocin (Jo et al., 1998) respectively. Neuropeptides also induce postsynaptic changes in neuronal electrical properties via activation or inhibition of voltage-dependent currents, thus modifying the excitability level of the postsynaptic neurone. However, a direct modulation of postsynaptic glutamate sensitivity has been reported in several cases. For example, depression of glutamate-induced responses has been observed in the presence of cortistatin (Vasilaki et al., 1999) or melanin concentrating hormone (Gao and van den Pol, 2001). Such neuropeptide/glutamate interactions are especially relevant in the hypothalamus. In particular, amongst many hypothalamic peptides able to efficiently modulate hypothalamic excitatory synaptic transmission (Dickson et al., 1993 ; Feleder et al., 1996 ; van den Pol et al., 1996, 1998 ; Kinney et al., 1998 ; Kombian et al., 2000), somatostatin [somatotropin release inhibiting factor, SRIF (Brazeau et al., 1973)] can either increase or decrease glutamate sensitivity (Gardette et al., 1995). This dual effect depends on the activation of either sst1 or sst2 SRIF receptor subtypes, respectively (Lanneau et al., 1998). However, little is known about the intracellular mechanisms implicated in the SRIF control of glutamate sensitivity besides the involvement of Gi/Go protein pathways (Boehm and Betz, 1997 ; Lanneau et al., 1998).

To better understand the mechanisms involved in the inhibitory effects of SRIF on hypothalamic glutamatergic neurotransmission, we focused our attention on sst2 receptor subtype and alpha-amino-3-hydroxy-5-methyl-4-isoxazolepropionate (AMPA) glutamate receptors (GluRs) in mediobasal hypothalamic (MBH) slices. This hypothalamic area was selected because it displays a dense network of somatostatinergic fibres (reviewed in

Tannenbaum and Epelbaum, 1999) and the localization of the sst2 receptor subtype on MBH neurones was thoroughly documented (reviewed in Dournaud et al., 2000). Moreover, glutamate is the main excitatory neurotransmitter in this area (van den Pol et al., 1990). In this study, we have analysed the effects of the sst2 agonist octreotide (Hoyer et al., 1995) on 1) electrically evoked synaptic responses in slices and, 2) on the currents induced by the rapid application of glutamatergic agonists in cultured neurones. Activation of sst2 receptor subtype decreased AMPA responses in hypothalamic neurones but this occured only with a concomitant activation of either N-methyl-D-aspartate (NMDA) or metabotropic (mGluRs) glutamate receptors and depended on intracellular calcium concentration.

Methods

All experimental procedures involving animals and their care were conducted in conformity with INSERM committee guidelines and according to the principles expressed in the declaration of Helsinki.

HYPOTHALAMIC SLICES Experiments were conducted in 1-2 month-old male Sprague-Dawley rats (Janvier, Genest St

Isle, France). Animals were anesthetized with halothane and killed by decapitation using a guillotine. The brain was rapidly removed from the skull and placed in a chilled (0-3°C) extracellular solution of the following composition (in mM): NaCl, 124; KCl, 3; $MgSO_4$, 1; $CaCl_2$, 2; $NaHCO_3$, 26; NaH_2PO_4, 1.25; glucose, 10 (gassed with 95% O2/5% CO2, pH 7.3, 310-320 mOsm). Coronal slices (400 µm-thick) of the hypothalamus, including the median eminence, were cut using a vibratome (Campden Instruments, Leicester, UK). Slices were maintained at 30°C for at least 1 h before recording, transferred to a submersion chamber mounted on the stage of an upright microscope (Zeiss Axioskop, Iena, Germany) and held with a nylon net. The slice was continuously perfused throughout the experiment with gassed (95% O2/5% CO2) extracellular solution at room temperature (20-25°C).

MEDIOBASAL CELL CULTURES Preparation of MBH cultures was adapted from Lanneau et al.

(2000b). Sprague-Dawley pregnant rats on the 17th day of gestation were anesthetized with halothane and killed by decapitation using a guillotine. A coronal slice was sampled from each fetus and further dissected in a ventrocaudal fragment containing MBH. Tissues were pooled and disrupted by mechanical trituration in PBS/Fœtal Calf Serum (5%) medium. The cell suspension was spun for 10 min at 650 g and the pellet resuspensed in a defined serum-free medium. Cells were then seeded on 35 mm Petri dishes, precoated with gelatin/poly-L-lysine and Fœtal Calf Serum, at a density of 3 MBH per dish (650 000 cells per dish). Cells were maintained in a 37°C, 7% CO2 humidified atmosphere, and treated from 5 days in vitro on with 1 µM cytosine arabinoside to block glial proliferation. The medium was changed twice a week. In such culture conditions, neurones represent more than 85% of the cell population.

ELECTROPHYSIOLOGICAL RECORDINGS In hypothalamic slices, patch clamp recording pipettes were made from thick-walled borosilicate glass capillaries (4-6 MΩ when filled with internal solution) using a Brown-Flaming horizontal pipette puller (Sutter Instrument Co, Novato, CA). Electrodes were filled with an internal solution of the following composition (in mM): KCH_3SO_4, 140; KCl, 6; $MgCl_2$, 2; HEPES, 10; EGTA, 1.1; lidocaine N-ethyl bromide (QX-314) 5, ATP-Na_2, 4; GTP0Na, 0.5; pH 7.3; 290-300 mOsm (adjusted with CsOH 0.1M), or for experiments in the presence of 1,2bis(2-aminophenoxy)ethane-tetraacetic acid (BAPTA) (in mM): KCH_3SO_4, 120; KCl, 6; $MgCl_2$, 2; HEPES, 10; BAPTA, 20; QX-314, 5, ATP-Na_2, 4; GTP-Na, 0.5; pH 7.3; 290-300 mOsm. The extracellular solution was perfused at 1-2 ml/min. Patch recording pipettes were connected to the headstage attached to a three-way piezo-electric micromanipulator (Burleigh, BFI Optilas, Evry, France) and neurones were recorded using the whole-cell configuration of the patch-clamp technique (Hamill et al., 1981). After the attainment of cell access, transmembrane voltages and currents were recorded using an Axopatch 1D amplifier (Axon Instruments, Foster City, CA), digitized using a Digidata 1200 interface (Axon Instruments) and stored on a computer. Delivery of command voltages, online analysis and storage of current data into data files were driven by the Acquis 1 software (CNRS,

Paris, France). Neurones were voltage-clamped to –70 mV unless otherwise stated and currents recorded at room temperature (20-25°C). Series resistance (10-30 MΩ) was routinely compensated (80%). Cell input resistance and membrane capacitance transients were monitored during the entire recording by applying a –10 mV voltage step (150 msec) before each stimulation. Cells that exhibited changes exceeding 15% during the recording period were rejected. Bipolar tungsten stimulating electrodes were placed in the dorsal area of the MBH region to activate synaptic inputs to the recorded neurones. In all experiments, stimuli (0.2-1 msec duration, 100-500 µA intensity, 0.06 Hz) were applied to construct baseline of postsynaptic responses and to measure the time-dependent effect of drugs. Theoritical reversal potentials of mixed Glutamate/GABA, GABA, Glutamate or AMPA synaptic responses were calculated using the GHK equation. These values were compared to measured mean reversal potentials corrected for junction potentials estimated by measuring the offset potential at the end of each recording. In mediobasal cell cultures, neurones were recorded using the whole-cell configuration of the patch-clamp technique (Hamill et al., 1981). Borosilicate patch-clamp electrodes (4-6 MΩ) were obtained by a two-stage pull on a horizontal electrode puller (BB-CH Mecanex, Geneva, Switzerland) and filled with the internal solution of the following composition (in mM) : KCH_3SO_4, 140 ; KCl, 6 ; $MgCl_2$, 2 ; HEPES, 10 ; EGTA, 1.1 ; GTP-Na 0.5 ; $ATPNa_2$, 4; pH 7.30, 280-300 mOsm or for, the BAPTA experiments, with the following composition (in mM): KCH_3SO_4, 120 ; KCl, 6 ; $MgCl_2$, 2 ; HEPES, 10 ; EGTA, 1.1 ; BAPTA, 20 ; GTP-Na 0.5 ; $ATPNa_2$, 4 ; QX-314, 5 ; pH 7.30 ; 280-300 mOsm. QX-314 was omitted from the internal medium during the study of mGluRs. The external recording medium, of the following composition (in mM) : NaCl, 140 ; KCl, 3 ; $CaCl_2$, 2 ; $MgCl_2$, 2 ; HEPES, 10 ; Glucose, 10 ; tetrodotoxin, $0.5.10^{-3}$; pH 7.30, 300-320 mOsm, was perfused at 2 ml/min. For the experiment without Ca^{2+} in the external medium, the diionic equilibrium of the solution was maintained using $BaCl_2$ 2 mM. Patch pipettes were mounted in the headstage attached to a three-way piezo-electric micromanipulator (Burleigh, BFI Optilas, Evry, France). After the attainment of cell access, transmembrane voltages and currents were recorded using an Axopatch 1D (Axon Instruments) amplifier, run on line using an Axon TL-1

DMA interface and stored on a computer. Delivery of command voltages and storage of current data into data files were driven by the Pclamp 6.0.4 software (Axon Instruments). Neurones were voltageclamped at –70 mV unless otherwise stated, and currents were recorded at room temperature (20-25°C). Series resistance (10-30 MΩ) was routinely compensated (80%). Cell input resistance and membrane capacitance transients were monitored as in hypothalamic slices.

DRUG APPLICATIONS Drug aliquots were dissolved in distilled water or DMSO ($\leq$ 0.1% final concentration in extracellular medium) and kept at –80°C.

In the hypothalamic slice preparation, drugs aliquots were dissolved in the external medium and applied by bath perfusion for at least 10 mn to obtain a steady-state bath concentration.

The following compounds were used : Bicuculline (Sigma, St Quentin-Fallavier, France) ; D-2-amino-5-phosphopentanoic acid (AP5, Tocris Cookson Ltd, Bristol, UK) ; 6-cyano-7-nitroquinoxaline-2 ,3-dione (CNQX; Tocris Cookson) ; 1,2,3,4-tetrahydro-6-nitro-2,3-dioxo-benzo[f]quinoxaline-7-sulfonamide (NBQX, Sigma) ; 1-(4-aminophenyl)-4-methyl-7,8-methyenedioxy-5H-benzodiazepine hydrochloride (GYKI 52466, Sigma). Octreotide 1 µM (SMS 201-995, gift from Novartis, Rueil-Malmaison, France) was used as a potent and long acting sst2 agonist (Hoyer et al., 1995). This compound is also a weak agonist for sst3 and sst5 receptors but sst5 receptor immunoreactivity has not been detected in the rat MBH (reviewed in Dournaud et al., 2000) and sst3 receptors can be excluded from classical pre or postsynaptic sites (reviewed in Schulz et al., 2000). In mediobasal cell cultures, drug aliquots were diluted in the extracellular medium to the desired concentrations. They were applied with a RSC-160 rapid solution changer (Bio-Logic, Claix, France). Currents generated by the glutamate receptor agonists L-Glutamate (Sigma), AMPA (Tocris Cookson), NMDA (Tocris Cookson) and trans-($\pm$)-1-amino-1.3cyclopentanedicarboxylic acid (trans-($\pm$)-ACPD, Tocris Cookson) were measured for a 2 sec application at 0.05 Hz. After acquisition of a 10 min baseline current amplitudes, octreotide 200 nM was continuously applied for 10 min. To evaluate the effect of the sst2 receptor agonist, a 2 sec application of glutamate agonist(s) plus

octreotide was delivered every 20 sec. For the study of NMDA responses, D-serine 20 µM was added to saturate the strychnineinsensitive glycine site of NMDA receptors (Mothet et al., 2000).

IMMUNOHISTOCHEMICAL CHARACTERIZATION OF RECORDED NEURONES IN HYPOTHALAMIC SLICES In some experiments, biocytin (0.5 mg/ml) was added to the recording solution. At the end of

the recording period, slices were fixed for 2 h in 4% paraformaldehyde in 0.1 M phosphate buffer (pH 7.4) and cryoprotected at 4° C in 30% buffered sucrose for 24 h. Serial sections (30 µm thick) were cut on a freezing microtome, collected in 0.1 M phosphate buffer and immediately processed for double labeling studies using either somatostatin or sst2A antibodies and biocytin revelation. For SRIF immunohistochemistry, slices were processed using a rabbit polyclonal antiserum directed against SRIF [antisomatostatin1-12 (code IS-7), a gift from Dr. G. Tramu, CNRS URA 339, Bordeaux, France]. To detect the sst2A receptor, which is the only sst2 isoform expressed in MBH neurones (Sarret et al., 1998), a fully characterized antiserum raised in rabbit against the C-terminal segment 330-369 of the sst2A receptor protein was used (Helboe et al., 1997, 1999 ; Csaba et al., 2001, 2002). Free-floating sections were incubated overnight at room temperature in 1:4000 anti-SRIF antibody or in

1:400 anti-sst2A antibody. SRIF and sst2A antibodies were diluted in 0.1M Tris buffer Saline pH 7.4 (TBS), containing 0.3% Triton X-100 and either 0.5% normal goat serum (NGS) or 0.5% normal donkey serum (NDS). SRIF antibodies were revealed by incubating sections for 45 min in 1:500 goat Cy3-conjugated anti-rabbit IgG (red fluorescent signal ; Jackson Immunoresearch, West Grove, PA) diluted in TBS containing 5% NGS and 0.3% Triton X

100. Sst2A receptor antibodies were revealed using 1:4000 donkey Cy3-conjugated antirabbit IgG (red fluorescent signal ; Jackson Immunoresearch, West Grove, PA) diluted in TBS containing 5% NDS and 0.3% Triton X-100. After several washes, sections were incubated for 45 min in 1:4000 Streptavidin FITC (green fluorescent signal ; Jackson Immunoresearch, West Grove, PA) diluted in TBS to reveal biocytin injected through the recording pipette. Sections were then rinsed in TBS,

mounted on glass slides and coverslipped with a Vectashield solution (Vector Laboratories). Sections were analyzed by Confocal Laser Scanning Microscopy using a TCS SP2 confocal imaging system equipped with Ar 488 nm and HeNe 543 nm lasers (Leica Microsystems, Heidelberg, Germany). Digital images were collected from a single optical plane using a 40x Plan-Apochromat oil-immersion lens (NA 1.25). Pinhole setting was 0.75 Airy unit (AU) for all images. For each optical section, double fluorescence images were acquired in sequential mode to avoid potential contamination by linkage specific fluorescence emission "cross talk".

SINGLE CELL MULTIPLEX RT-PCR OF SST mRNAs

Cells were first patched and cytoplasm harvested by applying a gentle negative pressure to the pipette. The tip of the pipette was then broken in a PCR sterile tube and submitted to retrotranscription for 1h at 37°C as already described (Lanneau et al., 2000b). The resulting 15µl sample was kept at –80°C. Coamplification of the cDNAs encoding the five sst1-5 somatostatinergic receptors was performed simultaneously. Primers were identical to primers used in a previous study (Table I in Lanneau et al., 2000b).

RT reaction products were first amplified in the presence of every primer (25 pmol each) in a 100 µl volume in an automatic thermocycler (Genius Techne, Cambridge, UK) during 20 cycles (94°C for 30 sec, 56°C for 30 sec, 72°C for 30 sec). An extension step was then performed at 72°C for 10 min. PCR products were purified from primers and salt using Nucleon QC microspin (Amersham, Rainham, UK).

A second round of PCR was then performed using 2 µl of the first purified PCR products as template. In this round, each marker was amplified individually using its specific primer pair for 28-35 cycles. All markers were amplified as described for the first amplification step. Amplification was performed in an automatic thermocycler (Hybaid, Teddington, UK) (94°C for 30 sec, 58-60°C for 30 sec, 72°C for 30 sec).

Fifteen microliters of each individual PCR reaction were then run on 2% agarose gel stained with Gel Star (FMC Bioproducts, Rockland, ME). In each experiment, cytoplasms with nucleus were

submitted to the entire protocol without reverse transcriptase. The intronic sequence of SRIF amplicon was never detected, thus ruling out genomic DNA contamination.

DATA ANALYSIS For each cell, amplitudes of evoked or induced currents were normalized relative to responses prior to drug application. Octreotide effect was estimated from amplitude mean decrease under drug in slices and from maximal mean decrease of steady-state currents in cultures. Statistical significance of amplitude variation within each cell was determined using a Student's t test and Bonferonni correction for small samples. Differences were considered significant if $p<0.05$. This procedure allowed recorded neurones to be classified in two different populations: octreotide-sensitive and octreotide-insensitive. Mean amplitudes of octreotide effect were then compared using ANOVA. Data are expressed as mean ± s.e.m.

Results

SYNAPTIC STIMULATIONS IN HYPOTHALAMIC SLICES Synaptic currents in response to electrical stimulation were recorded in 55 neurones in order to characterize mixed glutamate and γ-aminobutyric acid (GABA) responses (n=12, no antagonist), pure GABA (n=11, addition of CNQX and AP5), glutamate (n=14, addition of bicuculline), AMPA (n=6, addition of bicuculline and AP5) or NMDA (n=6, addition of bicuculline and CNQX) responses, and glutamate responses in presence of intracellular BAPTA (n=6, addition of bicuculline). NBQX (1μM) and GYKI 52466 (20μM) were applied in order to block AMPA receptors and reveal kainate currents (Kawai and Sterling, 1999 ; Chergui et al., 2000). In such conditions, complete blockade of the synaptic response was observed, even after high stimulation intensities or frequencies (Vignes and Collingridge, 1997), thereby ruling out the presence of a kainate synaptic component. Current voltage (I-V) curves were also obtained from 20 neurones in order to characterize the I-V relationship for each type of synaptic response. The observed reversal potentials were : -17 $\pm$ 4 mV for mixed glutamate/GABA responses (Fig 1A, n=4), -52 $\pm$ 2 mV for pure GABA responses (Fig 1B, n=8), +13 $\pm$ 5 mV for pure glutamate responses (Fig

1C, n=5), and 12 ± 6 mV for AMPA responses (Fig 1D, n=3), in agreement with calculated GHK reversal potentials in our experimental conditions (GABA : -50 mV, glutamate : +13 mV, AMPA : +13 mV). As shown in Figure 2A and 2B, mixed glutamate/GABA synaptic responses were decreased by –28.8 ± 3.8 % under octreotide ($p<0.001$ vs control values before octreotide in responsive cells, n=5, and values under octreotide in non responsive cells, n=7). The octreotide effect took place about three minutes after the beginning of the perfusion and slowly increased during its application. No recovery was observed. To test whether octreotide affected specifically glutamate and/or GABA components of the synaptic responses, experiments were reproduced in the presence of either CNQX and AP5 (n=11) to isolate the GABA component, or bicuculline (n=14) to isolate the glutamate response. Octreotide had no effect on the GABA component (Fig 2C,D) whereas octreotide inhibited the glutamate component in 43% of the recorded neurones (6/14, fig 2E,F) with an average decrease of –32.3 ± 5.9 % ($p<0.001$ vs control values before octreotide in responsive cells, n=6, and values under octreotide in non responsive cells, n=8). The amplitude and kinetics of octreotide effects on glutamate responses were not significantly different from those observed for mixed glutamate/GABA responses. NMDA contribution to total glutamate current was estimated by applying AP5 and represented around 5% of the total synaptic current at a holding potential of –70 mV and in the presence of Mg^{2+} (1 mM) in the perfusion solution (data not shown). These results suggest that the sst2 agonist modulates mainly the AMPA component of the glutamate synaptic response. However, when the AMPA component was isolated by addition of both bicuculline and AP5, octreotide was ineffective at inhibiting the response in 6 out of 6 recorded neurones (fig 2G,H).

This led us to test whether an influx of calcium through NMDA channels might be required to observe octreotide effects. Indeed, octreotide modulation of glutamate synaptic responses was abolished by intracellular injection of BAPTA in every tested neurone (n=6, Fig 2I,J). To rule out a presynaptic inhibition of glutamate release related to calcium-induced release of a retrograde messenger from the postsynaptic cell, the effect of octreotide was tested on pharmacologically isolated NMDA synaptic currents (n=6). Holding potential was set to –20 mV to remove Mg^{2+} blockade and allow a larger

calcium influx. Under these conditions, no effect of octreotide was ever observed (data not shown).

As shown in Figure 3, recorded MBH neurones were surrounded by a dense network of somatostatinergic fibers in close apposition to neuronal perykarya and dendrites.

Regional examination of slices immunoreacted with the sst2A receptor antibody revealed that numerous immunopositive neurones were apparent throughout the MBH (data not shown). In accordance with previous studies (reviewed in Dournaud et al., 2000), the largest proportion of receptor-expressing cells was observed in the arcuate nucleus. At the cellular level, receptor immunolabeling was confined to small spherical granules displaying the morphological features of endosomes distributed at the periphery of the cells as well as within intracellular compartments. Such cellular distribution has been recently described in other brain regions and reflect activation and subsequent internalization of cell-surface sst2A receptors in response to agonist stimulation (Csaba et al., 2001, 2002). Combined electrophysiological recordings with double-labeling experiments revealed that biocytinfilled neurones displaying no octreotide-induced changes in glutamate synaptic currents never expressed sst2A receptor immunolabeling (Fig 4A-C) while responsive cells displayed sst2A receptor immunoreactivity (Fig 4D-F).

FAST APPLICATIONS OF AGONISTS IN MEDIOBASAL CELL CULTURES

The lack of effect of octreotide on the AMPA component of the synaptic response on the one hand, and the BAPTA blockade of octreotide-induced decrease of the glutamate synaptic response on the other hand, led us to determine whether a coactivation of non-NMDA and NMDA glutamate ionotropic receptor subtypes was necessary to observe the sst2 modulation of the AMPA responses. Indeed, the linearity of synaptic glutamate and AMPA I-V curves (see additional material) strongly suggested that the activated glutamate receptors contained the edited GluR2 subunit and were not permeable to calcium (Jonas et al., 1994). Experiments were performed on a total number of 78 isolated neurones in primary cultures allowing fast perfusion of the cells with octreotide and various glutamate agonists alone or in combination. In cells held to –70 mV and in the presence of 2 mM Mg^{2+}, the AMPA current

represented more than 95% of the total recorded inward current, thus indicating a 5% contribution of NMDA activation, similar to that recorded for synaptic responses in slices. As previously reported, at the agonist concentrations used herein, AMPA-mediated responses displayed no fast peak current (Swandulla et al., 1994). As shown in Figure 5A and 5B, the fast application of octreotide + glutamate decreased the glutamate-induced inward current in 43% of the tested neurones (3/7) with a maximum average decrease of –15.9 $\pm$ 4.1 % ($p<0.001$ vs control values before octreotide in responsive cells, n=3, and values under octreotide in non responsive cells, n=4). As opposed to slice experiments, octreotide effect desensitized rapidly before the end of application. Octreotide-induced decrease was also found when all glutamate receptor subtypes were activated by coapplying AMPA, NMDA and trans($\pm$)-ACPD in 38% of the tested cells (3/8) with a comparable maximum average decrease of –12.5 $\pm$ 0.4 % ($p<0.001$ vs control values before octreotide in responsive cells, n=3, and values under octreotide in non responsive cells, n=5 ; Fig 5C,D). Fast application of AMPA with octreotide on 9 cells never led to a decreased AMPA current (Fig 5E,F) while octreotide coapplied with AMPA and NMDA decreased the AMPA current by –8.4 $\pm$ 1.6 % ($p<0.001$ vs control values before octreotide in responsive cells, n=5, and values under octreotide in non responsive cells, n=8, Fig 5G,H). In a second series of experiments, we tested whether calcium influx through the coactivated NMDA receptors could be responsible for restoring octreotide modulation of the AMPA current. As shown in Figure 5I and 5J, omitting calcium from the extracellular medium totally abolished the decrease of AMPA current during coapplication of AMPA, NMDA and octreotide in all 15 tested neurones. However, octreotide was still able to decrease glutamate response by –14.1 $\pm$ 1.7 % in 3 out of 7 tested cells even in the absence of extracellular calcium (data not shown) suggesting that mGluRs were involved in sst2/AMPA receptor interactions.

ROLE OF METABOTROPIC GLUTAMATE RECEPTORS Experiments were performed in cultured neurones with no extracellular calcium. Agonist coapplications with octreotide included AMPA and

trans-(±)-ACPD in order to activate GluRs and mGluRs, respectively. Under these conditions, octreotide was effective in reducing AMPA current in 43% of the recorded neurones (3/7, Fig 6A,B) with a maximal effect of –
15.1 ± 3.5 % which desensitized rapidly. After intracellular perfusion of BAPTA, 3 out of 6 tested cells were still responsive to octreotide (Fig 6C,D), but the magnitude of the effect was significantly diminished (–7.8 ± 1.0 % vs –15.1 ± 3.5 % in the absence of BAPTA, $p<0.001$). Furthermore, a 45 minute preincubation with thapsigargin, to deplete intracellular calcium stores, totally abolished the effect of octreotide on AMPA currents elicited during a coapplication of AMPA and trans-(±)-ACPD (Fig 6E,F, n=6).

DISTRIBUTION OF SST mRNAs IN MBH CELL CULTURES Cytoplasms were harvested from 39 neurones from rat MBH cell cultures and were processed in order to detect expression of the five sst mRNAs at the single cell level. 31% (12/39) of the
neurones expressed no sst mRNAs. A same proportion of the cells (12/39) expressed only one subtype whereas the simultaneous expression of 2, 3, 4 or 5 subtypes was detected respectively in 26% (10/39), 8% (3/39), 5% (2/39) and 0% (0/39) of the neurones. The mRNA signal for the sst2 subtype was found in 49% of the neurones, in close agreement with the proportion of octreotide-sensitive cells. The distribution of the other mRNAs subtypes was as follows : sst4 (36%) > sst1 (28%) > sst5 (8%) > sst3 (5%).

Discussion

In this study, we first determined the role of the sst2 receptor subtype on synaptic transmission in rat MBH slices. Electrical stimulation of the dorsal part of MBH elicited mixed glutamatergic and GABAergic synaptic responses in all recorded neurones, in keeping with the major role attributed to these two amino acids in the hypothalamic network (van den Pol et al., 1990 ; Decavel and van den Pol,

1990). Sst2 modulation of the GABA component was never observed, suggesting that octreotide-induced decrease of mixed synaptic responses was entirely due to the effect of the peptide on the glutamate component. Such a lack of SRIF effect on GABAergic transmission has previously been reported in the hippocampus (Boehm and Betz, 1997 ; Tallent and Siggins, 1997). Glutamate responses were decreased by octreotide in 43% of the recorded neurones and octreotide sensitivity was correlated to the presence of sst2A receptor immunoreactivity. This proportion of octreotide sensitive neurons in MBH slices is in close agreement with the proportion of sst2 receptor-expressing neurones observed in culture by single cell RT-PCR in this study (49%) as well as in previous reports on mouse hypothalamic neurones (40%, Lanneau et al., 1998 ; 44%, Lanneau et al., 2000a). Octreotide modulation appeared mainly targeted to the AMPA component which represents the main component of fast excitatory transmission within the hypothalamus (Wuarin and Dudek, 1993).

The effect of octreotide appears unrelated to a depression of neurotransmitter release from presynaptic terminals (Boehm and Betz, 1997) since neither the postsynaptic NMDA component of the synaptic response nor GABA synaptic responses were affected by the peptide. A decrease in postsynaptic neuronal excitability, mediated by sst2-modulation of postsynaptic voltage-dependent ionic channels (reviewed in Patel, 1999), is also unlikely because such a decrease would have equally affected the amplitude of AMPA or GABA responses. Sst2-induced inhibition totally disappeared when the AMPA component was pharmacologically isolated. This indicates that, in such experimental conditions, one essential element between the sst2 receptors and the GluRs was missing. The main difference between non-selective glutamate-and selective AMPA-receptor mediated responses was the pharmacological blockade of NMDA receptors in the latter protocol. Indeed, octreotide inhibition of AMPA responses was restored in cultured neurones when NMDA was coapplied with AMPA.. Based on previously published reports demonstrating the expression of GluR2 mRNA in mediobasal hypothalamic areas (van den Pol et al., 1994; Eyigor et al., 2001) and given the linearity of AMPA I-V curves observed in both slices and isolated neurones, it appears most likely that native AMPA receptors expressed by hypothalamic neurones contained the edited GluR2 subunit and thus display no

calcium permeability (Burnashev et al., 1992; Jonas et al., 1994). Thus calcium fluxes through NMDA receptors may be necessary for the expression of the sst2-induced modulation of AMPA currents. In the slice experiments, involvement of mGluRs-induced calcium release from intracellular stores appeared unlikely since 1) these receptors are located at a distance from the synaptic zone and 2) they require higher frequencies of stimulation to be activated (Ottersen and Landsend, 1997).

The role of intracellular calcium in the sst2-induced modulation of AMPA current is supported by several arguments. When calcium was omitted from the extracellular medium in cultures, the effect of octreotide was abolished. When intracellular calcium was chelated by BAPTA, sst2-induced inhibition of glutamate synaptic responses was blocked. Moreover, in cultures, octreotide effect was restored by the coactivation of GluRs and mGluRs, strongly depressed by intracellular BAPTA and abolished by thapsigargin preincubation. This last observation suggested that calcium ions involved in the sst2-AMPA modulation pathway may arise indifferently from extracellular or intracellular sources. The fact that octreotide-induced inhibition of AMPA currents was restored even when coactivated NMDA currents represented, in our experimental conditions, only about 5% of total glutamate-mediated currents is rather surprising. Indeed, the calcium influx mediated by such a small amount of current is probably not very consequent. One hypothesis could be that calcium transients elicited by NMDA receptor activation are confined to a space near the site of entry (Yuste and Denk, 1995) leading to a very local rise in calcium-concentration sufficient to trigger intracellular events in a microdomain containing the different receptor subtypes. In keeping with this hypothesis, it has been recently shown that calcium transients restricted to the the immediate vicinity of the site of calcium entry represents the on switch for ERK1/2 kinase signaling independently of global increases in calcium concentration (Hardingham et al., 2001). Alternatively, this local calcium increase could be responsible for the onset of a calcium-induced calcium release mechanism, as shown in hippocampal dendritic spines (Emptage et al., 1999), leading to substantial calcium release from the internal stores close to glutamate and sst2 receptors and subsequent activation of intracellular messengers. Octreotide induced an equivalent decrease of AMPA currents when mGluRs alone, or mGluRs + NMDA

receptors together, are activated. This suggests that a mGluRs-induced increase in intracellular calcium alone can lead to a maximal effect of octreotide on AMPA transmission. Such a result may be highly relevant in the functioning of synaptic networks, especially in view of the putative corelease of glutamate and somatostatin (Lanneau et al., 2000b). During synaptic transmission with a low rate of action potential firing, AMPA and NMDA receptors are activated and only a modest release of neuropeptides occurs (Hökfelt, 1991). In this case, decrease of excitatory synaptic transmission by sst2 activation would be very low, due to a low level of activation of sst2 receptors by basal somatostatin release. An increase in the rate of action potential discharge, such as in kindling or status epilepticus, will lead to an enhanced release of both somatostatin (Manfridi et al., 1991 ; Vezzani et al., 1992) and glutamate from nerve terminals. In such conditions, the simultaneous activation of sst2 and mGluRs will result in a higher inhibition of excitatory transmission. Thus, activation of sst2 receptors may represent a physiological brake against overexcitation of synaptic networks. This hypothesis may be relevant to further define the mechanisms of the inhibitory role of somatostatin in seizures and epileptogenesis (Vezzani and Hoyer, 1999). We observed, in slices, a mean octrotide-induced depression of glutamate responses that was twice that observed in cultures neurones (32% versus 16%). This difference may be related to a release of maximal concentrations of glutamate when using evoked potentials in the slice, leading to maximal AMPA responses, whereas the low agonist concentration used in cultured neurones would activate only a subset of available AMPA receptors and induce a smaller excitatory current. This may lead to a less efficient effect of the sst2 agonist on the smaller glutamate responses. Alternatively, glutamate receptors activated during the fast application or the electrical-induced synaptic responses are differentially located on the postsynaptic cell. Thus, only synaptically-based receptors would respond to a single-shock electrical stimulation whereas both synaptically and extrasynaptically-located receptors would be activated when applying drugs. Such a differential receptor distribution at the neuronal surface leads to different regulation of receptor subtypes (Morishita et al, 2001). Thus, sst2 activation may lead to a larger octreotide-induced depression of synaptically-based receptors than of extrasynaptically-based ones, reflected by a more

potent effect of the sst2 agonist in slices than in cultures. The octreotide response desensitized rapidly in cultures as opposed to slices. Such a discrepancy between the slice and dispersed neurone protocols has previously been observed. For instance, inhibition of ICa by somatostatin in cultured chick sympathetic neurones desensitizes with a time for half desensitization of approximately 3 minutes (Golard et al., 1993), as observed in the present experiments in cultured hypothalamic neurones. On the opposite, Tallent and Siggins (1997) reported that somatostatin-induced depression of AMPA/kainate EPSCs in rat hippocampal slices did not desensitize in their recording conditions. Since somatostatin receptor desensitization was hypothetized to be dependent on receptor internalization rather than on phosphorylation events (Beaumont et al., 1998), the differences observed in desensitization kinetics between cultures and slices may be related to different internalization processes. Indeed, it has been shown in different culture systems that the maximal rate of rat sst2 internalization ranged between 50% and 95% (reviewed in Csaba and Dournaud, 2001) whereas it reaches only 20-30% in rat brain slices even after a 40 minute exposure to sst2 agonist (Boudin et al, 2000). Therefore, it is likely that the available number of membrane sst2 receptors is largely decreased in isolated cultured cells as compared to slices. This may explain the persistance of octreotide effect in slices as opposed to its rapid disappearance in isolated hypothalamic neurones. Previously reported effects of SRIF on neurotransmitter-activated receptors dealt with SRIFinduced changes of postsynaptic sensitivity and only involved two classes of postsynaptic receptors (reviewed in Vezzani and Hoyer, 1999). To our knowledge, only one example showed a true cooperativity between receptors : in SH-SY5Y human neuroblastoma cells, SRIF applied alone is ineffective on intracellular calcium levels whereas coapplication of SRIF and carbachol evoked an elevation above that caused by carbachol alone (Connor et al., 1997). However, cooperativity between several transmitters has already been shown, such as for serotonin, adenosine and SRIF in the coupling of their respective receptors to an inwardly rectifying potassium current (Sodickson and Bean, 1998). Such observations are in keeping with the present results where coactivation of three receptors is required to produce a biological effect (Figure 7). A link between intracellular calcium and the different ionotropic

glutamate receptor subtypes has recently been evidenced, such as the control of the targeting of GluR2-containing GluRs by Ca2+-permeable GluRs (Liu and Cull-Candy, 2000), or a transient depression of the kainate receptor current induced by Ca^{2+} influx through NRs (Ghetti and Heinemann, 2000). Interactions between receptors belonging to different families such as ionotropic and G protein-coupled receptors also exist. Thus, a rise of postsynaptic calcium is required for the induction of D1/D5-induced sustained enhancement of GluRs- and NRs-mediated currents (Yang, 2000). Given the broad spectrum of the intracellular targets modified by the increase in calcium ions, several hypotheses can be considered in the interaction between sst2 and glutamate receptors depending on intracellular calcium. Common intracellular targets to both intracellular calcium (reviewed in Berridge, 1998) and sst2 (reviewed in Csaba and Dournaud, 2001) mostly involve kinases or phosphatases such as the adenylate cyclase/cAMP/PKA (reviewed in Schindler et al., 1996) or the MAP kinase (reviewed in Cole and Schindler, 2000) pathways. An interaction between calcineurin phosphatase and sst receptors activated by SRIF-28 has also been described (Zhu and Yakel, 1997). Activation of these pathways in response to both sst2 and intracellular calcium may lead to phosphorylation or dephosphorylation of GluRs (reviewed in Greengard, 2001), a major mechanism in the regulation of neurotransmitter receptors (reviewed in Swope et al., 1992). For example, dephosphorylation of GluRs is observed during long term depression in the hippocampus, a phenomenon associated with a decrease in GluRs sensitivity (Lee et al., 1998). Interestingly, this NMDA-induced long term depression associated with dephosphorylation of GluRs can be observed after only a 3 minute application of NMDA, a delay compatible with our present observations (Lee et al., 1998). Alternatively, the sst2 receptor itself could be the target for phosphorylation or dephosphorylation following intracellular calcium rise (reviewed in Csaba and Dournaud, 2001), a mechanism that could account for changes in sst2 receptor properties allowing AMPA modulation. Finally, a direct interaction between sst2 receptor and GluRs, induced by intracellular calcium rise, could also account for the modifications of glutamate responses. Such a physical association has recently been demonstrated between dopamine D5 receptor subtype, a G protein-coupled receptor as

the sst2 receptor, and $GABA_A$ receptor subtype, a ligand-gated channel mediating fast interneuronal synaptic transmission analogous to GluRs (Liu et al., 2000). It has been demonstrated that sst2 can physically bind to proteins with anchoring and scaffolding functions (Zitzer et al., 1999). One of these proteins, named SSTRIP (sst receptor interacting protein, or SHANK1), also binds, directly or by other binding proteins, to NRs, mGluRs and GluRs (reviewed in Craig and Boudin, 2001). Therefore, this physical link may, under calcium control, modify AMPA sensitivity by a mechanism comparable to that of Homer proteins controlling constitutive activity of mGluR1a or mGluR5 receptors (Ango et al., 2001). In summary, the modulation of GluRs sensitivity by activation of the SRIF sst2 receptor subtype represents a complex mechanism under the control of intracellular calcium levels. The calcium rise is induced by Ca^{2+} influx through NMDA receptors and/or by calcium release from internal stores after mGluRs activation. These two pathways are most likely implicated in the modulation of glutamate sensitivity in different physiological conditions, either during normal synaptic transmission for NMDA receptors or in the case of excitatory hyperactivity for mGluRs. These results suggest an unsuspected regulatory mechanism involving at least three different receptor subtypes and bring a new level of interaction in the modulatory effects of neuropeptides on fast synaptic transmission.

References

Ango F., Prézeau L., Muller T., Tu J.C., Xiao B., Worley P.F., Pin J.P., Bockaert J. & Fagni L. (2001). Agonist-independent activation of metabotropic glutamate receptors by the intracellular protein Homer. *Nature* **411**, 962-965

Barker J.L., Neale J.H., Smith T.G. & Macdonald R.L. (1978). Opiate peptide modulation of amino acid responses suggests novel form of neuronal communication. *Science* **199**, 1451-1453

Beaumont V., Hepworth M.B., Luty J.S., Kelly E. & Henderson G. (1998). Somatostatin receptor densensitization in NG 108-15 cells. A consequence of receptor sequestration. *Journal of Biological Chemistry* **273**, 33174-33183

Behbehani M.M., Pun R.Y., Means E.D. & Anderson D.K. (1990). Thyrotropin-releasing hormone has profound presynaptic action on cultured spinal cord neurons. *Synapse* **6**, 169-174

Berridge M.J. (1998). Neuronal calcium signaling. *Neuron* **21**, 13-26

Bijak M. (2000). Neuropeptide Y reduces epileptiform discharges and excitatory synaptic transmission in rat frontal cortex *in vitro*. *Neuroscience* **96**, 487-494

Boehm S., Betz H. (1997). Somatostatin inhibits excitatory transmission at rat hippocampal synapses via presynaptic receptors. *Journal of Neuroscience* **17**, 4066-4075

Boudin H., Sarret P., Mazella J., Schonbrunn A. & Beaudet A. (2000). Somatostatininduced regulation of SST_{2A} receptor expression and cell surface availability in central neurons : role of receptor internalization. *Journal of Neuroscience* **20**, 5932-5939

Brazeau P., Vale W., Burgus R., Ling N., Butcher M., Rivier J. & Guillemin R. (1973).

Hypothalamic polypeptide that inhibits the secretion of immunoreactive pituitary growth hormone. *Science* **179**, 77-79

Burnashev N., Monyer H., Seeburg P.H. & Sakmann B. (1992). Divalent ion permeability of AMPA receptor channels is dominated by the edited form of a single subunit. *Neuron* **8**, 189-198

Chergui K., Bouron A., Normand E. & Mulle C. (2000). Functional GluR6 kainate receptors in the striatum : indirect down regulation of synaptic transmission. *Journal of Neuroscience* **20**, 2175-2182

Cole S.L. & Schindler M. (2000). Characterisation of somatostatin sst2 receptor splice variants. *Journal of Physiology (Paris)* **94**, 217-237

Connor M., Yeo A. & Henderson G. (1997). Neuropeptide Y Y2 receptor and somatostatin sst2 receptor coupling to mobilization of intracellular calcium in SH-SY5Y human neuroblastoma cells. *British Journal of Pharmacology* **120**, 455-463

Craig A.M. & Boudin H. (2001). Molecular heterogeneity of central synapses : afferent and target regulation. *Nature Neuroscience* **4**, 569-578

Csaba Z., Bernard V., Helboe L., Bluet-Pajot M.T., Bloch B., Epelbaum J. & Dournaud P. (2001). In vivo internalization of the somatostatin sst2A receptor in rat brain: evidence for translocation of cell-surface receptors into the endosomal recycling pathway. *Mol. Cell. Neurosci.* **17**, 646-661

Csaba Z. & Dournaud P. (2001). Cellular biology of somatostatin receptors. *Neuropeptides* **35**, 1-23

Csaba Z., Simon A., Helboe L., Epelbaum J. & Dournaud P. (2002). Neurochemical characterization of receptor-expressing cell populations by in vivo agonist-induced internalization: insights from the somatostatin sst2A receptor. *J. Comp. Neurol.* in press

Decavel C. & van den Pol A.N. (1990). GABA : a dominant neurotransmitter in the hypothalamus. *Journal of Comparative Neurology* **302**, 1019-1037

Dickson S.L., Leng G. & Robinson I.C.A.F. (1993). Systemic administration of growth hormone-releasing peptide activates hypothalamic arcuate neurons. *Neuroscience* **53**, 303306

Dournaud P., Slama A., Beaudet A. & Epelbaum J. (2000). *Somatostatin receptors*. In: Handbook of Chemical Neuroanatomy,Volume 16 : Peptide receptors Part I (Quirion R, Björklund A, Hökfelt T, eds.), pp 1-43. Amsterdam: Elsevier

Emptage N., Bliss T.V.P. & Fine A. (1999). Single synaptic events evoke NMDA receptor-mediated release of calcium from internal stores in hippocampal dendritic spines. *Neuron* **22**, 115.124

Eyigor O., Centers A. & Jennes L; (2001) Distribution of ionotropic glutamate receptor subunit mRNAs in the rat Hypothalamus. *J. Comp. Neurol.* **21**, 101-124

Feleder C., Jarry H., Leonhardt S., Moguilevsky J.A. & Wuttke W. (1996). Evidence to suggest that gonadotropin-releasing hormone inhibits its own secretion by affecting hypothalamic amino acid neurotransmitter release. *Neuroendocrinology* **64**, 298-304

Gao X.B. & van den Pol A.N. (2001). Melanin concentrating hormone depresses synaptic activity of glutamate and GABA neurons from rat lateral hypothalamus. *Journal of Physiology (Lond.)* **533**, 237-252

Gardette R., Faivre-Bauman A., Loudes C., Kordon C. & Epelbaum J. (1995). Modulation by somatostatin of glutamate sensitivity during development of mouse hypothalamic neurons in vitro. *Developmental Brain Research* **86**, 123-133

Ghetti A. & Heinemann S.F. (2000). NMDA-dependent modulation of hippocampal kainate receptors by calcineurin and Ca^{2+}/calmodulin-dependent protein kinase. *Journal of Neuroscience* **20**, 2766-2773

Golard A., Role L.W. & Siegelbaum S.A. (1993). Protein kinase C blocks somatostatin-induced modulation of calcium current in chick sympathetic neurons. *J. Neurophysiol.* **70**, 1639-1643

Greengard P. (2001). The neurobiology of slow synaptic transmission. *Science* **294**, 1024-1030

Hamill O.P., Marty A., Neher E., Sakmann B. & Sigworth F.J. (1981). Improved patchclamp techniques for high-resolution current recording from cells and cell-free membrane patches. *Pflügers Archiv* **391**, 85-100

Hardingham G.E., Arnold F.J.L. & Bading H. (2001). A calcium microdomain near NMDA receptors : on switch for ERK-dependent synapse-to-nucleus communication. *Nature Neuroscience* **4**, 565-566

Helboe L., Hay-Schmidt A., Stidsen C.E. & Moller M. (1999). Immunohistochemical localization of the somatostatin receptor subtype 2 (sst2) in the central nervous system of the golden hamster (Mesocricetus auratus). *J Comp Neurol* **405**, 247-261

Helboe L., Moller M., Norregaard L., Schiodt M. & Stidsen C.E. (1997). Development of selective antibodies against the human somatostatin receptor subtypes sst1-sst5. *Brain Res Mol Brain Res* **49**, 82-88

Hökfelt T. (1991). Neuropeptides in perspective : the last ten years. *Neuron* **7**, 867-879

Hoyer D., Bell G.I., Berelowitz M., Epelbaum J., Feniuk W., Humphrey P.P.A., O'Carroll A.M., Patel Y.C., Schonbrunn A., Taylor J.E. & Reisine T. (1995). Classification and nomenclature of somatostatin receptors. *Trends in Pharmacological Sciences* **16**, 86-88

Jo Y.H., Stoeckel M.E., Freund-Mercier M.J. & Schlichter R. (1998). Oxytocin modulates glutamatergic synaptic transmission between cultured neonatal spinal cord dorsal horn neurons. *Journal of Neuroscience* **18**, 2377-2386

Jonas P., Racca C., Sakmann B., Seeburg P.H. & Monyer H. (1994). Differences in Ca^{2+} permeability of AMPA-type glutamate receptor channels in neocortical neurons caused by differential GluR-B subunit expression. *Neuron* **12**, 1281-1289

Kawai F. & Sterling P. (1999). AMPA receptor activates a G-protein that suppresses a cGMP-gated current. *Journal of Neuroscience* **19**, 2954-2959

Kinney G.A., Emmerson P.J. & Miller R.J. (1998). Galanin-receptor mediated inhibition of glutamate release in the arcuate nucleus of the hypothalamus. *Journal of Neuroscience* **18**, 3489-3500

Kombian S.B., Mouginot D., Hirasawa M. & Pittman Q.J. (2000). Vasopressin preferentially depresses excitatory over inhibitory synaptic transmission in the rat supraoptic nucleus in vitro. *Journal of Neuroendocrinology* **12**, 361-367

Lanneau C., Viollet C., Faivre-Bauman A., Loudes C., Kordon C., Epelbaum J. & Gardette R. (1998) Somatostatin receptor subtypes sst1 and sst2 elicit opposite effects on the response to glutamate of mouse hypothalamic neurones : an electrophysiological and single cell RT-PCR study. *European Journal of Neuroscience* **10**, 204-212

Lanneau C., Bluet-Pajeot M.T., Zizzari P., Csaba Z., Dournaud P., Helboe L., Hoyer D., Pellegrini E., Tannenbaum G.S., Epelbaum J. & Gardette R. (2000a). Involvement of the sst1 somatostatin receptor subtype in the intrahypothalamic neuronal network regulating Growth Hormone secretion : an in vitro and in vivo antisense study. *Endocrinology* **141**, 967-979

Lanneau C., Peineau S., Petit F., Epelbaum J. & Gardette R. (2000b). Somatostatin modulation of excitatory synaptic transmission between periventricular and arcuate hypothalamic nuclei in vitro. *Journal of Neurophysiology* **84**, 1464-1474

Lee H.K., Kameyama K., Huganir R.L. & Bear M.K. (1998). NMDA induces long-term synaptic depression and dephosphorylation of the GluR1 subunit of AMPA receptors in hippocampus. *Neuron* **21**, 1151-1162

Liu F., Wan Q., Pristupa Z.B., Yu X.M., Wang Y.T. & Niznik H.B. (2000). Direct protein-protein coupling enables cross-talk between dopamine D5 and γ-aminobutyric acid A receptors. *Nature* **403**, 274-280

Liu S.Q.J. & Cull-Candy S.G. (2000). Synaptic activity at calcium-permeable AMPA receptors induces a switch in receptor subtype. *Nature* **405**, 454-457

Manfridi A., Forloni G.L., Vezzani A., Froditto F. & De Simoni M.G. (1991). Functional and histological consequences of quinolinic and acid-induced seizures on hippocampal somatostatin neurons. *Neuroscience* **41**, 127-135

Mazarati A.M., Hohmann J.G., Bacon A., Liu H., Sankar R., Steiner R.A., Wynick D. & Wasterlain C.G. (2000). Modulation of hippocampal excitability and seizures by galanin. *Journal of Neuroscience* **20**, 6276-6281

McQuiston A.R. & Colmers W.F. (1996). Neuropeptide Y_2 receptors inhibit the frequency of spontaneous but not miniature EPSCs in CA3 pyramidal cells of rat hippocampus. *Journal of Neurophysiology* **76**, 3159-3168

Morishita W., Connor J.H., Xia H., Quinlan E.M., Shenolikar S. & Malenka R.C. (2001). Regulation of synaptic strength by protein phosphatase 1. *Neuron* **32**, 1133-1148

• Mothet J.P., Parent A.T., Wolosker H., Brady R.O. Jr, Linden D.J., Ferris C.D., Rogawski

M.A. & Snyder S.H. (2000). D-serine is an endogenous ligand for the glycine site of the N-methyl-D-aspartate receptor. *Proceedings of the National Academy of Sciences of the USA* **97**, 4926-4931

Ottersen O.P. & Landsend A.S. (1997). Organization of glutamate receptors at the synapse. *European Journal of Neuroscience* **9**, 2219-2224

Patel Y.C. (1999). Somatostatin and its receptor family. *Frontiers in Neuroendocrinology* **20**, 157-198

Sarret P., Botto J.M., Vincent J.P., Mazella J. & Beaudet A. (1998). Preferential expression of sst2A over sst2B somatostatin receptor splice variant in rat brain and pituitary. *Neuroendocrinology* **68**, 37.43

Schindler M., Humphrey P.P. & Emson P.C. (1996). Somatostatin receptors in the central nervous system. *Progress in Neurobiology* **50**, 9-47

Schulz S., Häendel M., Schreff M., Schmidt H. & Höllt V. (2000). Localization of five somatostatin receptors in the rat central nervous system using subtype-specific antibodies. *Journal of Physiology (Paris)* **94**, 259-264

Sodickson D.L. & Bean B.P. (1998). Neurotransmitter activation of inwardly rectifying potassium current in dissociated hippocampal CA3 neurons : interactions among multiple receptors. *Journal of Neuroscience* **18**, 8153-8162

Swandulla D., Zeilhofer H.U., Misgeld U. & Beckh S. (1994). Functional and molecular characteristics of the glutamate receptor involved in synaptic transmission in the hypothalamus. *Ann. Rev. New Acad. Sci. USA* **733**, 163-173

Swope S.H., Moss S.J., Blackstone C.D. & Huganir R.L. (1992). Phosphorylation of ligand-gated ion channels : a possible mode of synaptic plasticity. *FASEB Journal* **6**, 2514-2523

Tallent M.K. & Siggins G.R. (1997). Somatostatin depresses excitatory but not inhibitory neurotransmission in rat CA1 hippocampus. *Journal of Neurophysiology* **78**, 3008-2018

Tannenbaum G.S. & Epelbaum J. (1999). *Somatostatin*. In: Handbook of Physiology Volume 5 : Hormonal Control of Growth (Kostyo J.L. Volume ed. ; Goodman H.M., Section ed.), pp 221-265. New-York: Oxford UP.

van den Pol A.N., Wuarin J.P. & Dudek F.E. (1990). Glutamate, the dominant excitatory transmitter in neuroendocrine regulation. *Science* **250**, 1276-1278

van den Pol A.N., Hermans-Borgmeyer I., Hofer M., Ghosh P. & Heinemann S. (1994). Ionotropic glutamate-receptor gene expression in hypothalamus : localization of AMPA, Kainate, and NMDA receptor RNA with in situ hybridization. *J. Comparative Neurology* **343**, 428-444

van den Pol A.N., Obrietan K., Chen G. & Belousov A.B. (1996). Neuropeptide Ymediated long-term depression of excitatory activity in suprachiasmatic nucleus neurons. *Journal of Neuroscience* **16**, 5883-5895

van den Pol A.N., Gao X.B., Obrietan K., Kilduff T.S. & Belousov A.B. (1998). Presynaptic and postsynaptic actions and modulation of neuroendocrine neurons by a new hypothalamic peptide, hypocretin/orexin. *Journal of Neuroscience* **18**, 7962-7971

Vasilaki A., Lanneau C., Dournaud P., De Lecea L., Gardette R. & Epelbaum J. (1999). Cortistatin affects glutamate sensitivity in mouse hypothalamic neurons through activation of sst2 somatostatin receptor subtype. *Neuroscience* **88**, 359-364

Vezzani A., Monno A., Rizzi M., Galli A., Barrios M. & Samanin R. (1992). Somatostatin release is enhanced in the hippocampus of partially and fully kindled rats. *Neuroscience* **51**, 41-46

Vezzani A. & Hoyer D. (1999). Brain somatostatin : a candidate inhibitory role in seizures and epileptogenesis. *European Journal of Neuroscience* **11**, 3767-3776

Vignes M. & Collingridge G.L. (1997). The synaptic activation of kainate receptors. *Nature* **388**, 179-182

Wuarin J.P. & Dudek F.E. (1993). Patch-clamp analysis of spontaneous synaptic currents in supraoptic neuroendocrine cells of the rat hypothalamus. *Journal of Neuroscience* **13**, 2323-2331

Yang S.N. (2000). Sustained enhancement of AMPA receptor- and NMDA receptormediated currents induced by D1/D5 receptor activation in the hippocampus : an essential role of postsynaptic Ca^{2+}. *Hippocampus* **10**, 57-63

Yuste R. & Denk W. (1995). Dendritic spines as basic functional units of neuronal integration. *Nature* **375**, 682-684

Zhu Y. & Yakel J.L. (1997). Calcineurin modulates G-protein-mediated inhibition of N-type calcium channels in rat sympathetic neurons. *Journal of Neurophysiology* **78**, 11611169

Zitzer H., Hönck H.H., Bächner D., Richter D. & Kreienkamp H.J. (1999). Somatostatin receptor interacting protein defines a novel family of multidomain proteins in human and rodent brain. *Journal of Biological Chemistry* **274**, 32997-33001

Acknowlegdements : We thank Dr Faivre-Bauman and Dr Loudes for the microdissection technique, Dr Csaba for helpful assistance during immunohistochemical processing, Dr Tramu for providing the somatostatin antibody, Dr Helboe for gift of the sst2A antibody, and Dr Davis for careful reading of the manuscript. This work was supported by INSERM, CNRS and QLG-1999-0908 european grant to JE. SP was a recipient of a fellowship from the French Research Ministery.

Figure 1 : Electrophysiological and pharmacological characterization of evoked synaptic responses in mediobasal hypothalamic slices.

(A) Current-voltage plot of synaptic responses. Membrane potential was clamped at –70 mV to +10 mV, at 10 mV steps. The reversal potential was –17 $\pm$ 4 mV (n=4). Synaptic responses (1) were partially blocked by bath application of ionotropic glutamate receptor antagonists CNQX 10µM and AP5 50µM (2). CNQX and AP5-resistant response was totally blocked by addition of the $GABA_A$ antagonist bicuculline 10µM (3).

(B) Current-voltage plot of GABAergic synaptic responses recorded in the presence of CNQX 10µM and AP5 50µM. Membrane potential was clamped at –70 mV to -30 mV, at 10 mV steps. The reversal potential was –52 $\pm$ 2 mV (n=8). The synaptic response (1) was totally blocked by bath application of bicuculline 10µM (2).

(C) Current-voltage plot of glutamatergic synaptic responses recorded in the presence of bicuculline 10µM. Membrane potential was clamped at -70 mV to +30 mV, at 10 mV steps. The reversal potential was 13 $\pm$ 5 mV (n=5). Synaptic responses (1) were totally blocked by bath application of CNQX 10µM and AP5 50µM (2).

(D) Current-voltage plot of AMPA synaptic responses recorded in the presence of bicuculline 10µM and AP5 50µM. Membrane potential was clamped at -70 mV to +30 mV, at 10 mV steps. The reversal potential was 12 $\pm$ 5 mV (n=3). Synaptic responses (1) were totally blocked by bath application of NBQX 1µM and GYKI 52466 20µM (2). Each trace in insets was obtained by averaging 3 responses. Scale bars 50 pA, 20 ms **Figure 2** : Effect of the sst2 receptor agonist octreotide on the amplitude of evoked synaptic responses in mediobasal hypothalamic slices.

(A) Time plot of normalized evoked synaptic responses. Five neurones displayed a highly significant decreased synaptic response during octreotide application () and 7 neurones were unresponsive (■).

(B) Average recording of 3 synaptic current traces before (CTRL) and during octreotide application (OCT) in one responsive neurone.

(C) Time plot of normalized evoked GABAergic synaptic responses. Synaptic responses were unaffected by octreotide in 11 tested neurone (■).

(D) Average recording of 3 GABAergic synaptic current traces in one neurone before (CTRL) and during octreotide application (OCT).

(E) Time plot of normalized evoked glutamatergic synaptic responses. Synaptic responses

were highly significantly depressed under octreotide application in 6 neurones () and unaffected in 8 neurones (■).

(F) Average recording of 3 glutamatergic synaptic current traces before (CTRL) and during octreotide application (OCT) in one responsive neurone.

(G) Time plot of normalized evoked AMPA synaptic responses. None of the 6 tested neurones showed a depressed synaptic response during octreotide application (■).

(H) Average recording of 3 AMPA synaptic current traces in one neurone before (CTRL) and during octreotide application (OCT).

(I) Time plot of normalized evoked glutamatergic synaptic responses in the presence of the calcium chelator BAPTA in the recording pipette. None of the 6 tested neurones showed depression of synaptic responses during octreotide application (■).

(J) Average recordings of 3 glutamatergic synaptic current traces in one neurone before (CTRL) and during octreotide application (OCT) in the presence of intracellular BAPTA. Scale bars : 50 pA, 10 ms

Figure 3 : Dense somatostatinergic innervation of recorded mediobasal hypothalamus neurones.

(a) The recording area (*, bleaching due to image acquisition) is included in a dense network of somatostatinergic fibres. (b) Biocytin revelation by FITC-labelled streptavidin of a recorded cell. (c) Somatostatinergic fibres in the vicinity of the recorded neurone. (d) Merged images of b and c illustrates the dense network of somatostatinergic fibres surrounding the recorded neurone. (e) single focal acquisition showing the presence of close appositions between somatostatinergic fibres and the neuronal perikaryon or dendrites (arrows). Scale bars : 200 µm in a, 10 µm in b (applies to b,c,d) and e ; ARC, arcuate nucleus ; ME, median eminence ; VMH, ventromedial hypothalamic nucleus ; 3V, third ventricle.

Figure 4 : Correlation between octreotide sensitivity and sst2A receptor expression (A-D) A : Average recording of 3 glutamatergic synaptic current traces before (CTRL) and during octreotide application (OCT) in one biocytin-injected unresponsive MBH neurone. Revelation of both biocytin (B) and sst2A receptor immunoreactivity (C) show the absence of sst2A receptor expression by the recorded neurone (D). (E-H) E : Average recording of 3 glutamatergic synaptic current traces before (CTRL) and during octreotide application (OCT) in one biocytin -injected responsive MBH neurone. Double labeling experiments indicate that the recorded neurone (F) displayed sst2A receptor immunoreactivity (G,H). Scale bars : a : 50 pA, 20 ms ; e : 40 pA, 5 ms ; d, h : 4 µm(applies to b-d and f-g).

Figure 5 : Effect of the sst2 receptor agonist octreotide on the activation of glutamate receptors in mediobasal hypothalamic cultures.

(A) Time plot of normalized glutamate-induced responses. 3 neurones presented a highly significant depression of the response during octreotide application () and 4 neurones were unresponsive (■).

(B) Recordings of glutamate-induced currents before (CTRL) and during octreotide application (OCT) in one responsive neurone.

(C) Time plot of normalized responses to coapplication of AMPA, NMDA and trans(±)-ACPD. Three neurones showed a highly significant depression of the responses during octreotide application () and five neurones were unaffected (■).

(D) Recordings of AMPA/NMDA/trans(±)-ACPD currents before (CTRL) and during octreotide application (OCT) in one responsive neurone.

(E) Time plot of normalized AMPA-induced responses. No change in the response was observed under octreotide in 9 tested neurones (■).

(F) Recordings of AMPA-induced currents in one neurone before (CTRL) and during octreotide application (OCT).

(G) Time plot of normalized responses to coapplication of AMPA and NMDA. Five neurones showed a highly significant depression of the responses during octreotide application () and 8 neurones were unaffected (■).

(H) Recordings of AMPA/NMDA currents before (CTRL) and during octreotide application (OCT) in one responsive neurone.

(I) Time plot of normalized responses to coapplication of AMPA and NMDA in the absence of external calcium. No depression of AMPA/NMDA responses was observed in the presence of octreotide in any of 15 tested neurones (■).

(J) Recordings of AMPA/NMDA currents in one neurone before (CTRL) and during octreotide application (OCT) in the absence of external calcium.

Each trace was fitted by a spline curve with a uniform local average smoother of span 100.

Scale bars : 20 pA, 1 s

Figure 6 : Role of group I mGluRs in sst2-evoked AMPA depression in mediobasal hypothalamic cultures.

(All experiments were performed in the absence of extracellular calcium)

(A) Time plot of normalized responses to coapplication of AMPA and trans-(±)-ACPD. 3 neurones displayed a highly significantly decreased response during octreotide application () and 4 neurones were unresponsive (■).

(B) Recordings of AMPA/trans-(±)-ACPD currents before (CTRL) and during octreotide application (OCT) in one responsive neurone.

(C) Time plot of normalized responses to coapplication of AMPA and trans-(±)-ACPD with BAPTA in the recording pipette. The inhibitory effect of octreotide was highly significantly decreased in 3 neurones () as compared to its effect in the absence of BAPTA (a).

(D) Recordings of AMPA/trans-(±)-ACPD currents in the presence of BAPTA before (CTRL) and during octreotide application (OCT) in one responsive neurone.

(E) Time plot of normalized responses to coapplication of AMPA and trans-(±)-ACPD following a thapsigargin pretreatment. No inhibitory effect of octreotide could be detected in 6 tested neurones (■).

(F) Recordings of AMPA/trans-(±)-ACPD currents in one neurone after thapsigargin pretreatment before (CTRL) and during octreotide application (OCT).

Each trace was fitted by a spline curve with a uniform local average smoother of span 100.

Scale bars : 20 pA, 1 s

Figure 7 : Schematic representation of sst2/AMPA interactions through intracellular calcium modifications.

During synaptic transmission, release of glutamate (Glu) from nerve endings activate AMPA (GluRs) and NMDA (NMDARs) receptors, as well as, when synaptic activity increases,

metabotropic glutamate receptors (mGluRs). The activation of NMDA receptors and/or mGluRs induces an increase in intracellular calcium concentration (Ca^{2+}). Calcium sources can be either extracellular, ions flowing through NMDA receptors, or intracellular, ions being released from endoplasmic reticulum (ER) following activation of the inositol phosphate pathway (IP) by mGluRs. Simultaneously, somatostatin (SRIF), released from identical or different nerve terminals, activates sst2 receptors (sst2). The activation of Gi/Go protein coupled-sst2 receptors induces a decrease in the

amplitude of glutamate-induced AMPA currents. If intracellular calcium concentration does not increase, sst2-modulation of GluRs does not occur. Thus, the amplitude of the sst2-induced inhibitory modulation depends on intracellular calcium levels. Putative links between calcium, sst2 and GluRs, are shown in the inset.

(P) = phosphorylation/dephosphorylation sites.

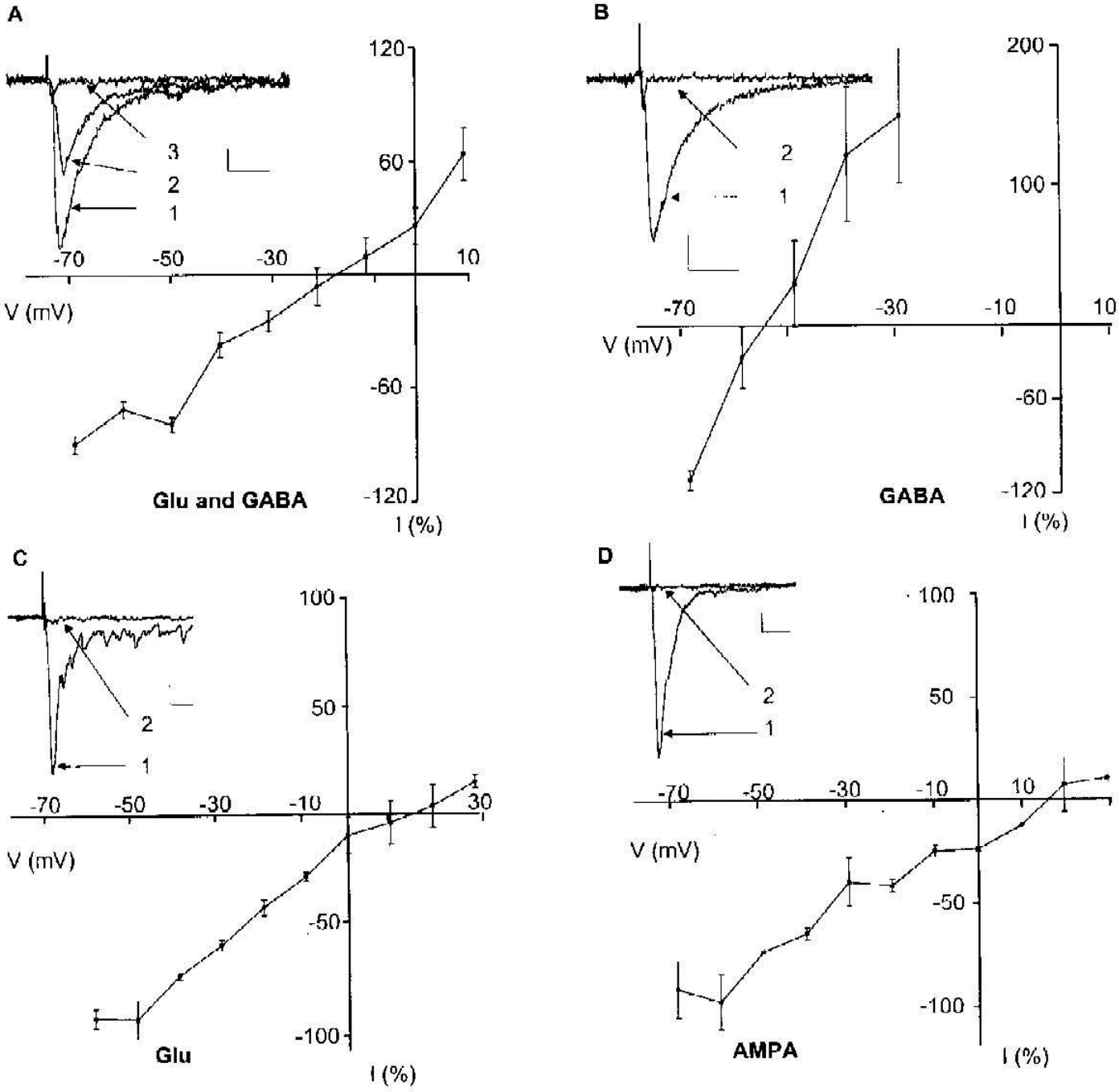
A
120
60
-60
-120
3
2
1
-70
-50
-30
10
V (mV)
Glu and GABA
I (%)
B
200
100
-60
-120
2
1
-70
-30
-10
10
V (mV)
GABA
I (%)
C
100
50
-50
-100
2
1
-70
-50
-30
-10
30
V (mV)
Glu
I (%)
D
100
50
-50
-100
2
1
-70
-50
-30
-10
10
V (mV)
AMPA
I (%)

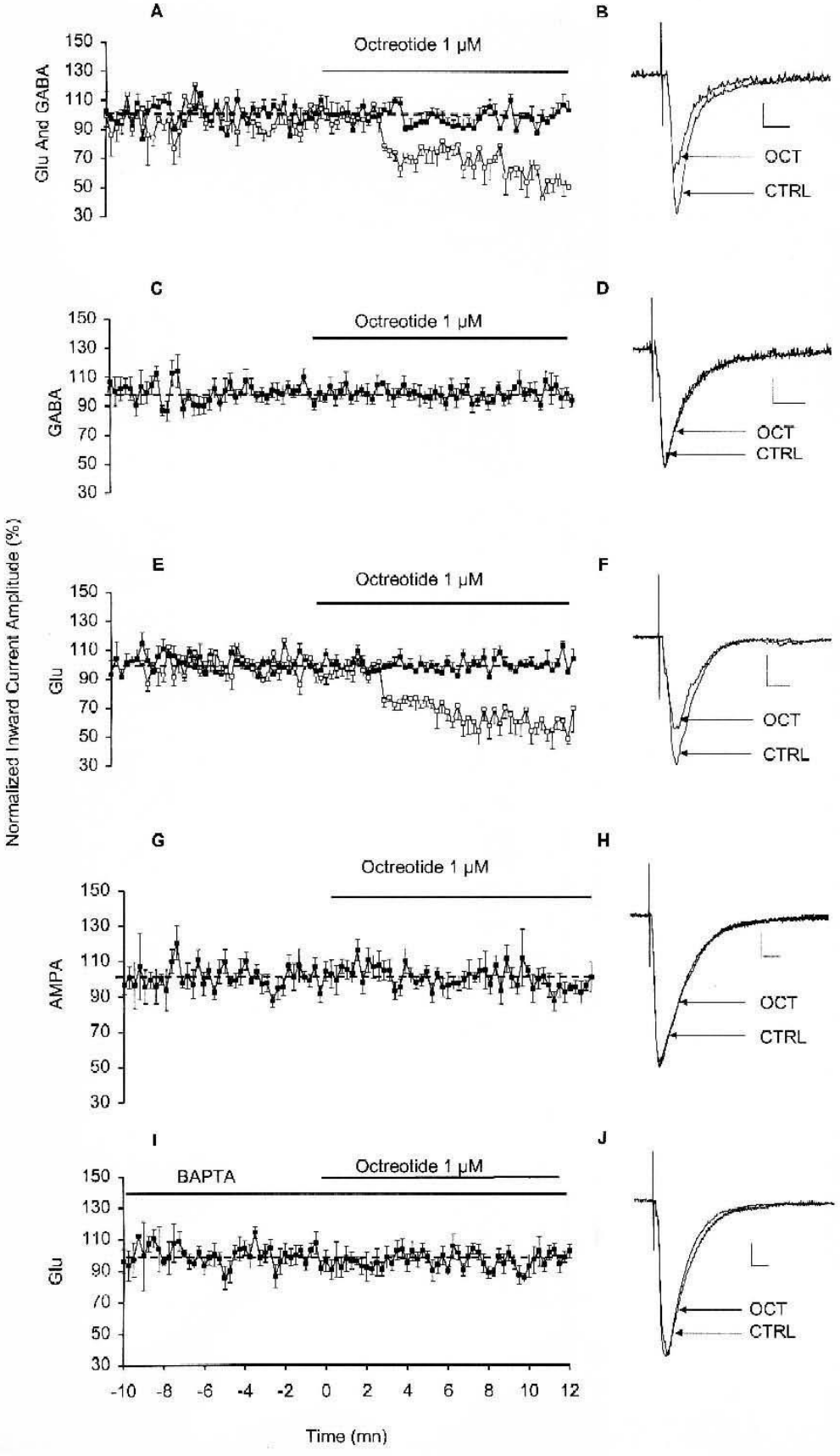
A
B
Octreotide 1 µM
Glu And GABA
OCT
CTRL
C
D
Octreotide 1 µM
GABA
OCT
CTRL
E
F
Octreotide 1 µM
Glu
OCT
CTRL
G
H
Octreotide 1 µM
AMPA
OCT
CTRL
I
J
BAPTA
Octreotide 1 µM
Glu
OCT
CTRL
150
130
110
90
70
50
30
-10 -8 -6 -4 -2 0 2 4 6 8 10 12
Time (mn)
Normalized Inward Current Amplitude (%)

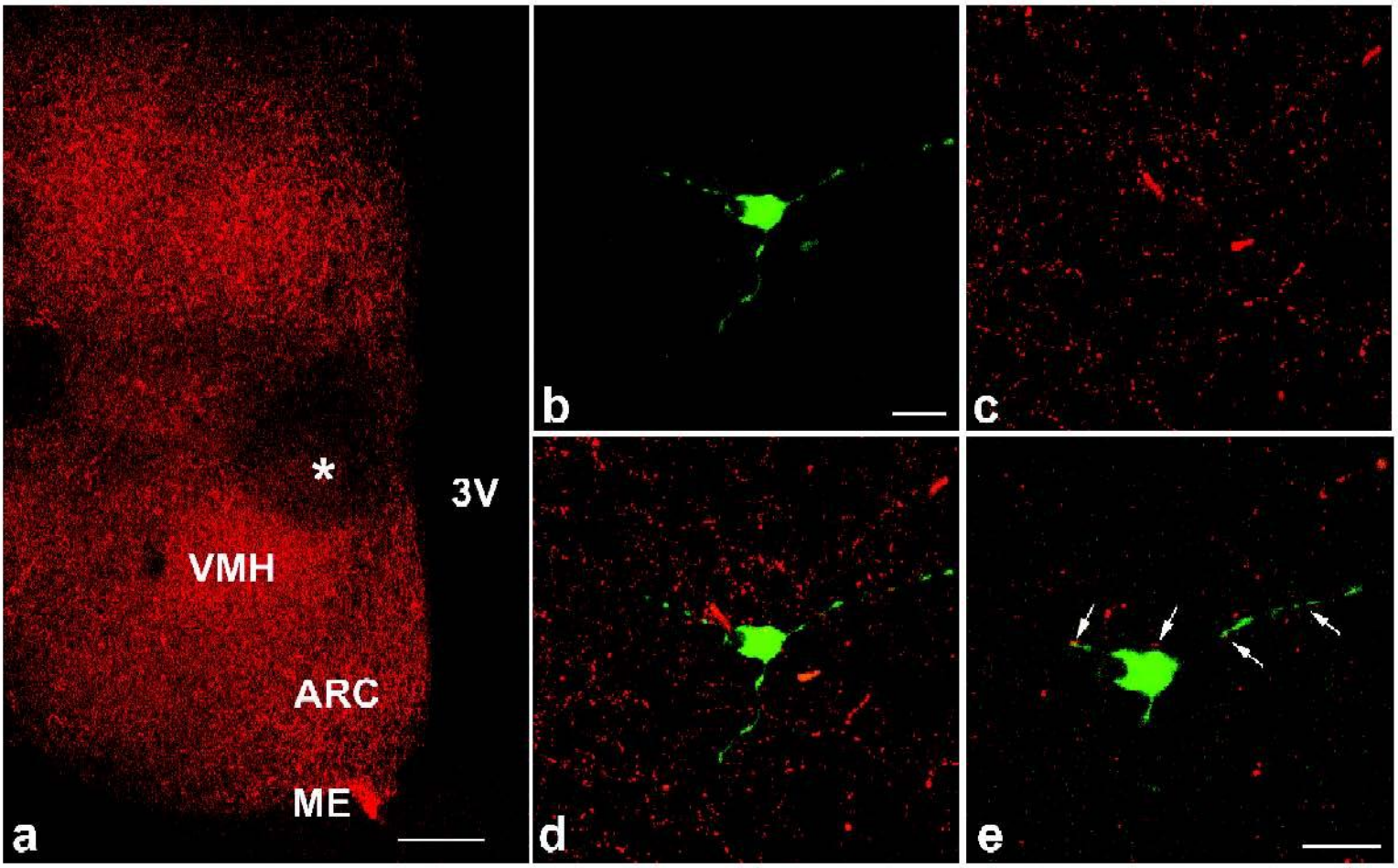
a
*
3V
VMH
ARC
ME
b
c
d
e

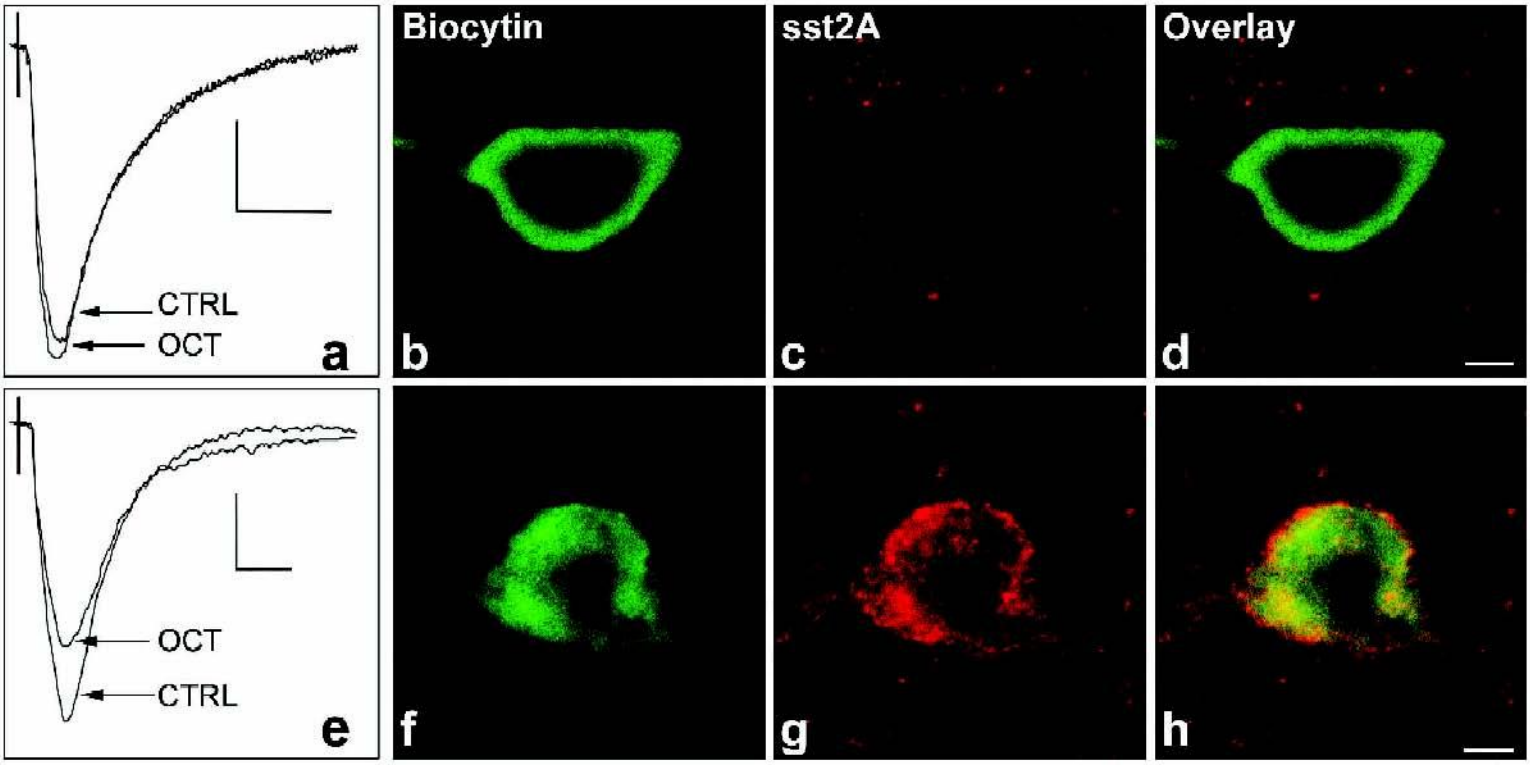
CTRL
OCT
a
Biocytin
b
sst2A
c
Overlay
d
OCT
CTRL
e
f
g
h

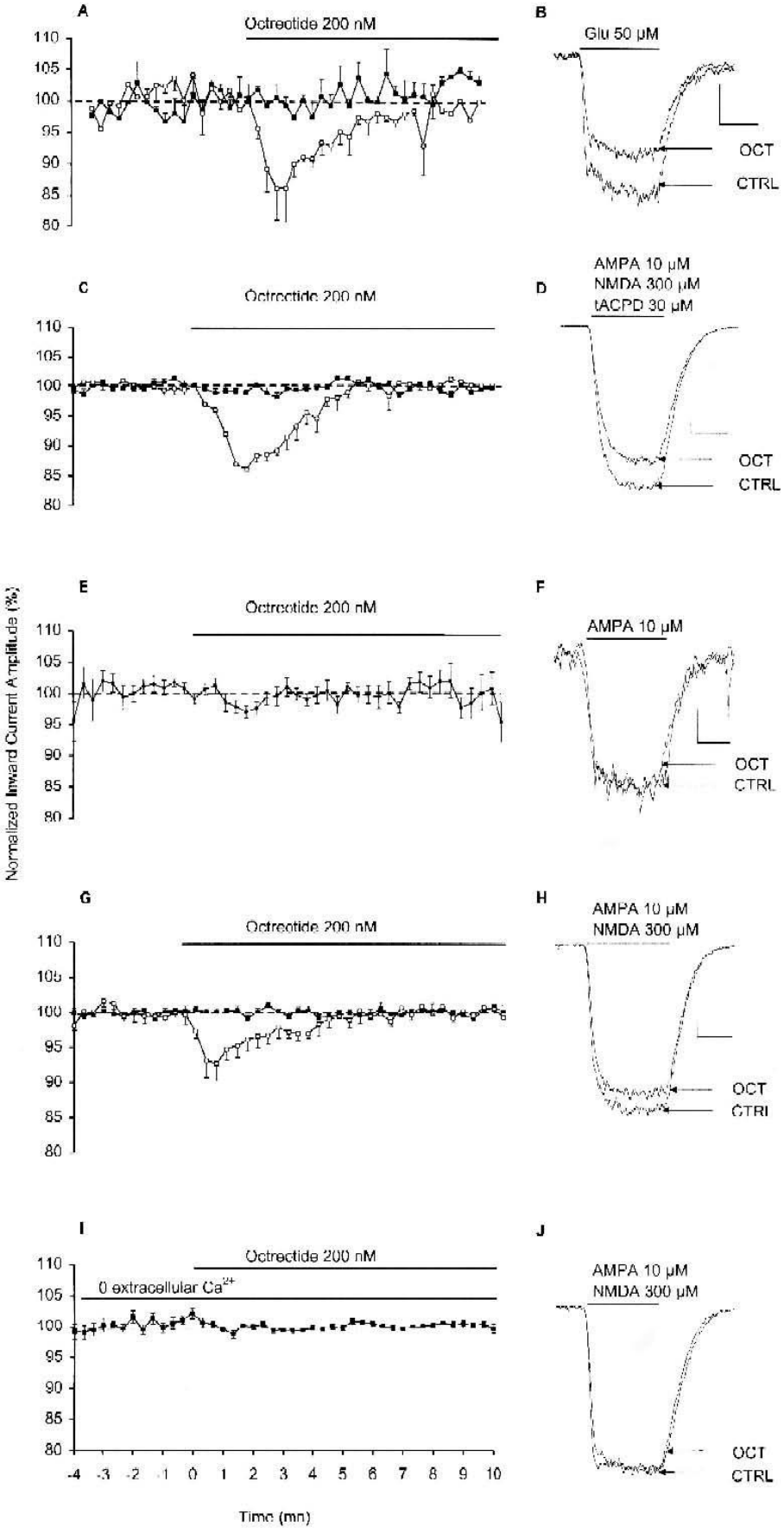
A
Octreotide 200 nM
B
Glu 50 µM
OCT
CTRL
C
Octreotide 200 nM
D
AMPA 10 µM
NMDA 300 µM
tACPD 30 µM
OCT
CTRL
E
Octreotide 200 nM
F
AMPA 10 µM
OCT
CTRL
G
Octreotide 200 nM
H
AMPA 10 µM
NMDA 300 µM
OCT
CTRL
I
Octreotide 200 nM
0 extracellular Ca2+
J
AMPA 10 µM
NMDA 300 µM
OCT
CTRL
Normalized Inward Current Amplitude (%)
110
105
100
95
90
85
80
-4 -3 -2 -1 0 1 2 3 4 5 6 7 8 9 10
Time (mn)

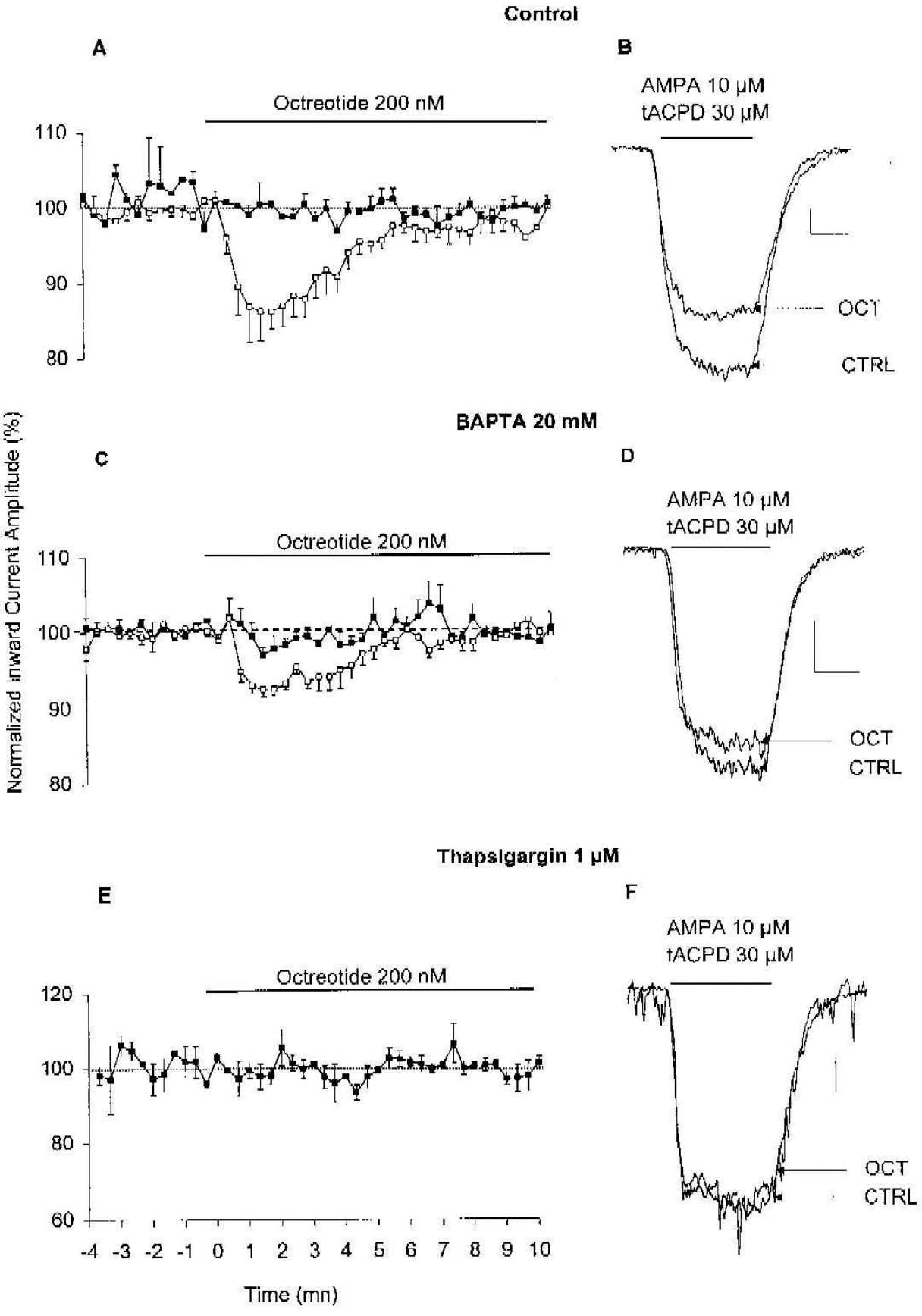
Control
A
Octreotide 200 nM
110
100
90
80
B
AMPA 10 µM
tACPD 30 µM
OCT
CTRL
BAPTA 20 mM
C
Octreotide 200 nM
110
100
90
80
D
AMPA 10 µM
tACPD 30 µM
OCT
CTRL
Normalized inward Current Amplitude (%)
Thapsigargin 1 µM
E
Octreotide 200 nM
120
100
80
60
-4 -3 -2 -1 0 1 2 3 4 5 6 7 8 9 10
Time (mn)
F
AMPA 10 µM
tACPD 30 µM
OCT
CTRL

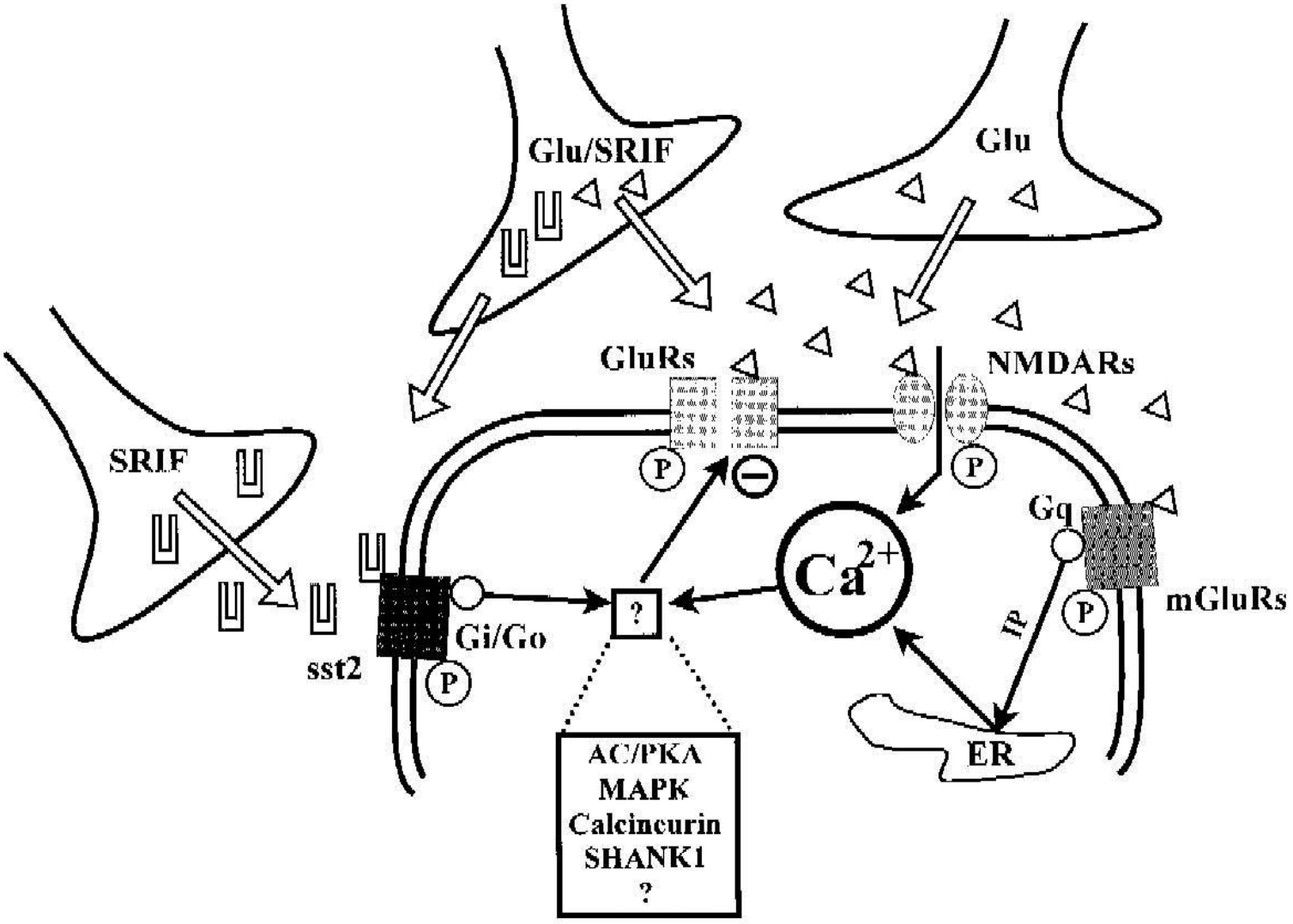
Glu/SRIF
Glu
GluRs
NMDARs
SRIF
P
Gq
mGluRs
Ca2+
Gi/Go
?
sst2
P
IP3
P
ER
AC/PKA
MAPK
Calcineurin
SHANK1
?